# Weather-based Loading of Overhead Lines – Consideration of Conductor's Heat Capacity

Thanos Krontiris, Andreas Wasserrab and Gerd Balzer
Institute of Electrical Power & Energy
Technische Universität Darmstadt
Landgraf-Georg-Str. 4, Darmstadt, D-64283
Email: thanos.krontiris@eev.tu-darmstadt.de

***Abstract*—Power transmission capacity of overhead lines is limited by the maximal conductor temperature: should this maximal temperature be exceeded, unacceptable line sag as well as increased ageing of the conductor itself could result. This is especially the case for the most common steel reinforced conductors, where grease –used for protection against corrosion– may leak at high temperatures.**

**Aside from the carried current, conductor temperature largely depends on the actual weather conditions: wind speed, ambient temperature as well as solar radiation may influence the thermal behaviour of a conductor at different rates.**

**According to actual standards, adverse weather conditions are taken as a basis when determining the maximal current for normal operation, which is then characteristic for an overhead line. However, if precise knowledge of actual weather conditions is available, the current constraint may be adapted leading to higher utilisation of the overhead line.**

**Usually, such information is given by weather forecasts and features an immanent forecast uncertainty. Moreover, it might be advantageous from an operational point of view to adapt the current constraint for a defined time interval in advance (e.g. for the next one hour), as this information has to be implemented into the settings of the protection system.**

**In order to account for these uncertainties, the volatility of weather parameters depending on the forecast horizon should be examined. Moreover, the question, whether short-term variations of weather conditions could lead to unacceptable conductor temperature rise, has to be answered.**

**Dynamic investigation of the thermal behaviour of overhead lines is therefore performed in this work, with special focus on the conductor's heat capacity. Additionally, steady-state calculations are performed and the results of both approaches (dynamic and steady-state) are compared. It is then possible to evaluate a safety margin for the calculated current constraint. A detailed thermal investigation of an Aluminum Conductor Steel Reinforced (ACSR) is given as a case study.**

## I. INTRODUCTION

The current carrying capacity of an overhead line (also called *ampacity*) is limited by following factors:

Overhead conductors feature a characteristic temperature threshold, depending on the deployed materials. In case this temperature threshold is exceeded, irreversible ageing of the corrosion protection system may occur, resulting in shortening of the conductor's lifetime. Protection against corrosion is usually provided by a grease coating. The maximal conductor temperature is then given by the dropping temperature of the protective grease, as specified in [9]. The carried current leads to a temperature rise of the conductor, mainly because of resistive losses. Accordingly, the current must be limited, in order to ensure that the conductor's temperature remains under the respective threshold during normal as well as fault operation.

Moreover, line sagging also depends on conductor temperature and, thus, on the carried current: the higher the operating current, the higher will the temperature be. The temperature rise leads to an elastic elongation of the conductor; in other words, line sagging increases. However, a voltage-specific ground clearance of the line has to be met at any time, so as to ensure that no flashover to adjacent objects may occur. For this reason, the operating current of an overhead line has to be limited.

### A. Temperature models

Aside from the carried current, conductor temperature largely depends on the actual weather conditions: wind speed and direction, ambient temperature as well as solar radiation may influence the thermal behaviour of a conductor at different rates. Several methods on calculating heat transfer and ampacities of transmission line conductors exist [1], [2]. In general, a rise of conductor temperature may be caused by following factors:

$$\text{Heat Gain Rate} = P_J + P_M + P_S + P_I \qquad (1)$$

The terms in equation 1 account for following factors:

- $P_J$ (Joule heating): Resistive losses due to current flow are the main driver for conductor heating during line operation. When evaluating the dc resistance of composite conductors (e.g. steel reinforced conductors), the non-uniform distribution of current density as well as the different temperature coefficients should be taken into account. Furthermore, it is usually also necessary to consider the skin effect, too.
- $P_M$ (Magnetic heating): In ACSR conductors, the aluminum wires are twisted around the steel core. This results in an axial magnetic flux during ac operation, which may induce eddy currents in the ferromagnetic core. Moreover, losses due to hysteresis can lead to conductor heating. However, magnetic losses are usually negligible for normal power frequency.
- $P_S$ (Solar heating): For precise calculation of solar heating, numerous parameters are relevant, e.g. the conductor's

inclination to the horizontal or the intensity of the direct as well as diffuse solar radiation. Many of these parameters are variable: for example, an overhead line does not have a constant orientation and also direct/diffuse solar radiation may be largely influenced by the atmosphere (passing clouds). It is therefore more practical to evaluate solar heating using only global solar radiation.

$P_I$ (Corona heating): Heating may also be caused by ionisation of the insulating medium (air) in close proximity to the conductor (Corona ionisation). The rate of Corona heating depends mainly on surface voltage gradient, which in turn in influenced by atmospheric precipitation. However, high precipitation will also result in increased cooling effects (see "water evaporation" below); thus, this heating factor is usually neglected.

On the other hand, cooling (or heat loss) effects are given by equation 2:

$$\text{Heat Loss Rate} = P_C + P_R + P_W \tag{2}$$

The terms in equation 2 stand for:

$P_C$ (Convective cooling): High conductor surface temperature results in heating of the air adjacent to the conductor. Depending on wind speed, two cases should be outlined regarding convection: in case of natural convection –when wind speed equals zero– heated air rises leading to natural air mass flow. On the other hand, when forced convection takes place, heated air is carried away by the forced mass flow. In both cases, colder air flows in to replace the heated air, thus cooling the conductor [1]. Forced convection provides the main cooling effect for overhead lines.

$P_R$ (Radiative cooling): Further heat losses occur by thermal radiation, depending on conductor surface temperature. Weathered conductors feature a higher emissivity constant than newer ones, which leads to higher radiative losses. Solar heating will, however, also be increased for the former conductors. Due to the relatively low operating temperature of overhead lines, radiative cooling usually plays only a minor role, especially if forced convection is apparent.

$P_W$ (Cooling due to water evaporation): Water evaporation may also contribute to conductor cooling in case of wet conductors. However, evaporative heat losses are generally ignored, mainly due to two reasons: first, atmospheric precipitation is not constant and, secondly, increased evaporative cooling in case of high precipitation is counteracted by increasing Corona heating.

Exact calculation formulae for the above heating as well as cooling factors may be found in [1]. The main input variables are: conductor core as well as surface temperature, $T_c$ and $T_s$ respectively, carried current, $I$, wind speed and angle of attack, $v_w$ and $\theta_w$, ambient temperature, $T_{amb}$, as well as global solar radiation, $I_S$.

## B. *Weather-based loading*

The maximal ampacity of overhead lines may be evaluated by steady-state (or quasi-steady-state) calculation. For this purpose, equations 1 and 2 have to be set equal.

According to DIN EN 50182 following values are provided for the weather parameters in the case of Germany [8]:

$T_{amb}$ : The ambient temperature is assumed to be $35\,^{o}$C.

$v_w$ : Wind speed is set equal $0.6$ m/s perpendicularly to the conductor (angle of attack $\theta_w = 90^o$).

$I_S$ : Global solar radiation is assumed as $900\,\text{W/m}^2$.

Obviously, the aforementioned weather conditions are adverse: the average ambient temperature in Germany is much lower than $35\,^{o}$C, even during hot summer days, while wind speed is usually significantly higher than $0.6$ m/s, especially in the coastal region. As a result, conductor temperature will lie far below the maximum temperature threshold during normal operation. Increased utilisation of overhead lines by considering actual values of weather parameters rather than the adverse conditions assumed above stands therefore to reason. Several Cigré task forces have addressed the limitations of steady-state thermal rating in the past [1], [3], [4].

Implementation of weather-based loading for overhead power lines should be performed in three steps [6], [7]:

1) First, the overhead line has to be geographically mapped. In particular, information about orientation of the line, orography or any possibly apparent wind obstacles (e.g. dense vegetation) must be captured, in order to identify any potential hot-spots. These may result from local wind shadowing effects.
2) In a further step, all relevant weather parameters have to be measured. Ambient temperature and solar radiation are –in general– not sensitive to local conditions. On the other hand, wind speed and direction may well be influenced by local factors: care should be therefore taken when passing the measured values from the measurement station on the conductor's site.
3) Finally, the ampacity of the line should be calculated on basis of the measured weather parameters. The evaluated current threshold should be then compared with the current ratings of other relevant equipment (e.g. power and instrument transformers, switches, circuit breakers etc.). The lowest value should be then passed on to the protection system.

## C. *Goals of this study*

Information about weather conditions may be given either continuously in form of on-line measurements or by means of forecasting. On-line measurements provide precise information about a variable of interest at the time of occurrence. However, appropriate measuring as well as data transmission and data processing systems are therefore necessary, which go along with significant investment costs. On the other hand, forecasts estimate the expected value of a variable over a specified time interval (the so-called forecast horizon). Forecasted values may be directly obtained from a weather service.

This work focuses on weather-based loading of overhead lines in case an appropriate short-term (e.g. hourly updated) weather forecast is given. Usually only expected values of the variables of interest (wind speed, wind direction, ambient temperature or global solar radiation) will be provided by a forecast. Either of the following approaches may then be chosen in order to determine the applicable ampacity of the overhead line:

- Steady-state approach: As already described in section I-B, equations 1 and 2 have to be set equal for the steady state (or quasi-steady state). This results to a closed analytical solution for the adapted ampacity, according to equation 3 [2]:

$$I = \frac{P_C + P_R - P_S}{R(T_{av})} \quad (3)$$

  with $R(T_{av})$ being the ac conductor resistance at temperature $T_{av}$. The average conductor temperature may be evaluated from the core and surface temperature if the radial temperature distribution is considered [1]. Magnetic and ionisation heating as well as evaporative cooling have been neglected in equation 3.
- Dynamic (or unsteady-state) approach: Potential fluctuation of the weather conditions may, however, influence the thermal behaviour of the conductors, possibly leading to unacceptable temperatures within the forecast horizon, if the result of equation 3 is used. In order to account for such intermediate fluctuations, the thermal balance of the conductor in the unsteady state should be considered as described by equation 4 [1]:

$$mc\frac{dT_{av}}{dt} = P_J + P_S - P_C - P_R \quad (4)$$

  The term $mc$ accounts for the heat capacity of the conductor, $m$ being the mass density and $c$ the specific heat capacity. In the case of composite conductors (e.g. ACSR), the total heat capacity may be evaluated by summing up the different components.
  Two prerequisites are necessary when solving the differential equation 4: highly sampled weather data must be available and the initial condition (i.e. initial conductor temperature) has to be known. If forecasts in terms of expected values are provided, the first prerequisite is not fulfilled. A general representation of site-specific short-term fluctuations of the relevant weather parameters could be used instead.

It is the objective of this work to investigate the fluctuations of weather parameters within a short-term forecast horizon (one hour) and to provide a comparison of the aforementioned steady-state and dynamic calculation. As a result, safety factors accounting for potential short-term weather fluctuations may be determined on a probabilistic basis. If these safety factors are then applied to equation 3, it would be possible to use the faster steady-state approach for calculation purposes. For this purpose, measured weather parameters are analysed in section II with regard to their volatility. In a further step, a computer model for dynamic calculation of the conductor's temperature is implemented in MATLAB®. Its general layout is given in section III. Finally, section IV provides a case study for a typical ACSR conductor.

## II. Weather parameters

Changes in weather conditions may result from local, small-scale as well as from large-scale factors. One typical example of a small-scale impact is the coastal breeze, which is caused by the different thermal emissivity of sea/land combined with the cyclic change of solar radiation. Such local factors are usually predictable. On the other hand, large-scale phenomena are generated by the exchange of significant air masses due to temperature or humidity gradients and are –in general– non-predicable.

When investigating the stochastic nature of weather parameters for modelling purposes, several questions should be considered:

1) Is the fluctuation of the variables of interest significant within the forecast horizon? The probabilistic analysis should focus mainly on highly volatile weather parameters.
2) Are the various weather parameters cross-correlated in some way? If so, modelling each variable independently by means of individual **p**robability **d**ensity **f**unctions (pdf) is not permitted.
3) Does the fluctuation of a variable within a time interval depend on its average value? In that case, several pdfs should be determined for different ranges.
4) Furthermore, the given time series for the relevant weather parameters should be preliminary examined with regard to their time resolution: the measurement intervals must not exceed the characteristic thermal time constant of the overhead conductor (typical conductors have thermal time constants of 10-15 minutes [3]).

### A. Input data

The input weather data for all investigations in this paper has been captured at the measurement station FINO 1 in the North sea [11]. This was the first research platform erected 2003 by the Federal Republic of Germany so as to quantify the potential of wind power in front of the German coast.

Although weather conditions offshore are quite different than onshore (smaller temperature fluctuations between day and night, as well as smoother wind speed distribution due to favourable surface finish), FINO 1 has been chosen as input data source since it provides accurate, long-term time series for all relevant weather parameters with sufficient time resolution (time intervals of 10 minutes). In addition, all time series are available for download at the website of the research project [11].

Figures 1 to 3 show the courses of year 2006 for the global solar radiation, the ambient temperature and the wind speed, respectively. As may be seen, the first two variables show a clear seasonal dependence, while the wind speed seems to be random.

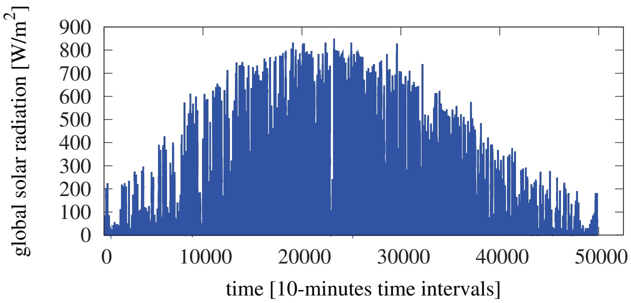


Fig. 1. Year course of global solar radiation [11]

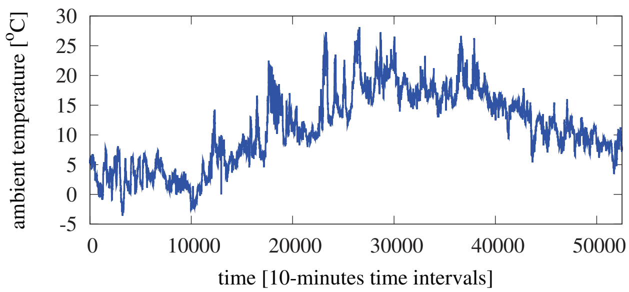


Fig. 2. Year course of ambient temperature [11]

It is obvious that the respective reference values for the global solar radiation ($900\text{W/m}^2$) and the ambient temperature ($35^{\text{o}}$C), as defined in [8], are not reached at any time. According to figure 2, the ambient temperature only varies between approximately $28^{\text{o}}$C and $-4^{\text{o}}$C. This is due to the thermal behaviour of the water surface in the North sea; significantly lower temperatures may be expected in the continental inland.

### *B. 10-minutes fluctuation of weather parameters*

In a further step, the short-term variation of the weather parameters is evaluated. For this purpose, every 10-minutes measurement is compared with its successive one and the difference is calculated. The results are given in figures 4 to 7 in form of cumulative probability diagrams (each diagram describes the probability that the fluctuation between successive measurements will not exceed a specified value, no matter the direction of the change –increase or decrease). In addition, the same procedure is repeated for the hourly mean values, as calculated by averaging six successive 10-minutes measurements.

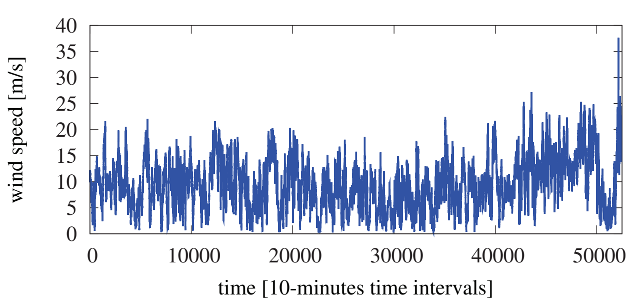


Fig. 3. Year course of the wind speed [11]

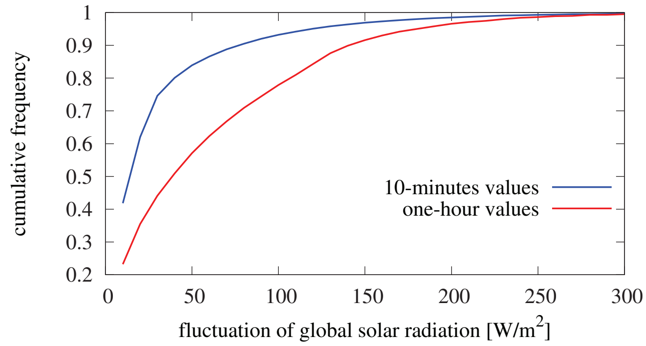


Fig. 4. Fluctuation of 10-minutes and one-hour measurements of the global solar radiation

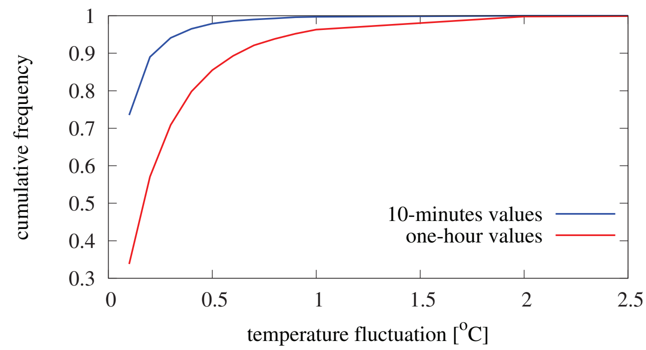


Fig. 5. Fluctuation of 10-minutes and one-hour measurements of the ambient temperature

The global solar radiation features high fluctuation, especially in the one-hour interval (the 90-percentile lies at approximately $140\text{W/m}^2$, compare figure 4). Nevertheless, the effect of solar heating is low compared to heating due to joule losses. It could be therefore advisable to use an appropriate constant value: for example, the maximal seasonal value observed in the past could be used as a reference.

From figure 5 it is obvious that the ambient temperature remains almost constant over an one-hour interval (the respective 90-percentile lies below $1^{\text{o}}$C). Modelling the stochastic nature of ambient temperature in the short-term is therefore not necessary.

On the other hand, wind speed seems to fluctuate significantly, as shown in figure 6: the 90-percentile of the hourly mean fluactuation exceeds 1.5m/s. The results shown in figure 6 have been evaluated without considering the absolute value of the wind speed. It is obvious that the parameter wind speed is subject to the highest fluctuation, compared with the other relevant weather parameters. Furthermore, the influence of wind speed on conductor temperature is large, due to forced cooling. A more precise investigation of wind speed volatility is therefore given in section II-D.

Finally, fluctuation of wind direction amounts approximately $20^{\text{o}}$ in an hourly basis (compare figure 7). Moreover, larger fluctuation is apparent at lower wind speeds where

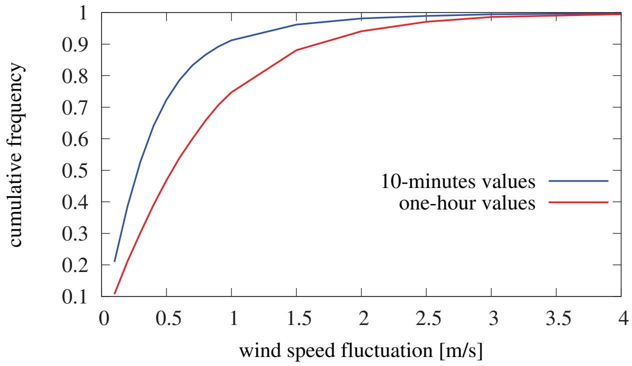


Fig. 6. Fluctuation of 10-minutes and one-hour measurements of the wind speed

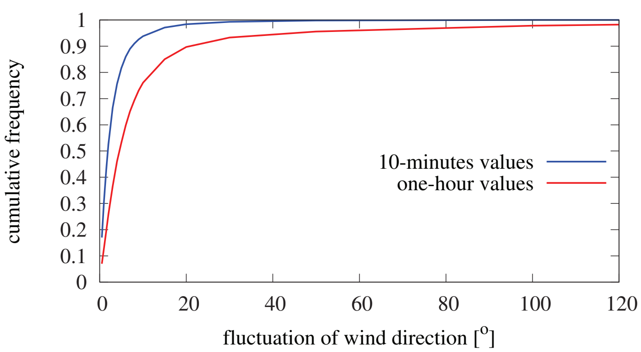


Fig. 7. Fluctuation of 10-minutes and one-hour measurements of the wind direction

convective cooling mainly occurs due to natural air mass flow [3]. Thus, it would be sufficient to assume a constant wind direction in the short term.

## C. Correlation of weather parameters

As already stated in section II, modelling the weather parameters by means of individual pdfs is only permitted if these are stochastically independent. The cross-correlation of two variables provides a practical and reliable measure of statistical dependence. Equation 5 defines the cross-correlation of variables $x$ and $y$ under consideration of a time lag $m$ ($\overline{x}$ and $\overline{y}$ are the respective mean values):

$$\rho_{xy}(m) = \begin{cases} \dfrac{\sum_{i=1}^{n-m}(x_{i+m}-\overline{x})(y_i-\overline{y})}{\sqrt{\sum_{i=1}^{n-m}(x_{i+m}-\overline{x})^2(y_i-\overline{y})^2}} & , \quad m \geq 0 \\ \rho_{yx} & , \quad m < 0 \end{cases} \tag{5}$$

In this section the dependence between ambient temperature and wind speed will be discussed. Although a relation between wind speed and ambient temperature is assumed in [3], with increasing temperatures leading to increasing wind speed, analysis of the given weather data did not verify this assumption. In figure 8, the cross-correlation between ambient temperature and wind speed for different time lags, $m$, is given. For $m = 0$ the cross-correlation index $\rho$ equals 0.1418, which indicates a weak statistical dependence. Furthermore, the value of the index does not change significantly for varying time

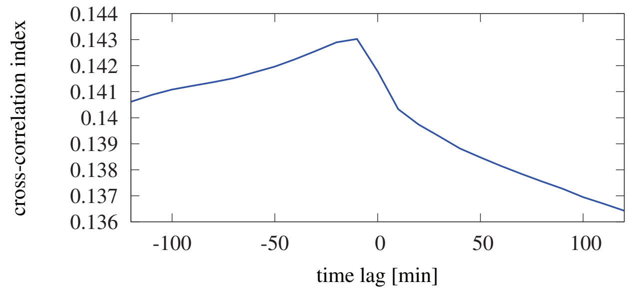


Fig. 8. Cross-correlation of wind speed and ambient temperature for different time lags

lags. Thus, modelling wind speed and ambient temperature as independent variables is justified for the given time series. Similar investigations have been performed also for the other relevant weather variables, however, no significant short-term statistical dependence between any of them could be identified.

## D. Wind volatility

Due to the large variations observed as well as due to its decisive role in the thermal behaviour of the conductor, wind speed has to be analysed in more detail. For this reason, the time series has been segmented in partitions of similar mean values (each partition had a spread of 1m/s), which were then analysed independently. Figure 9 shows the probability function for the various partitions. As expected, the absolute value of fluctuation increases with increasing wind speed. However, the *relative* fluctuation is lower for high wind speeds. The so-evaluated pdfs are used in section III for a probabilistic analysis on the basis of the dynamic thermal model (equation 4).

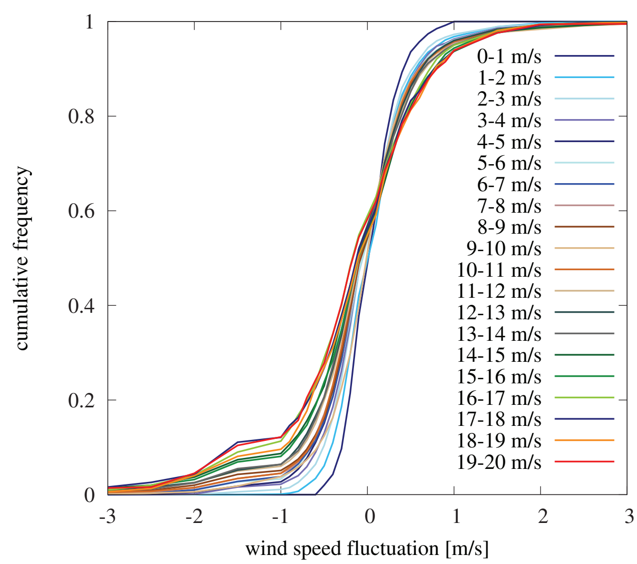


Fig. 9. Cumulative frequency of wind speed fluctuation on a 10-minutes basis

## III. Dynamic investigation of conductor temperature

A computer model has been developed in MATLAB® so as to simulate the thermal behaviour of overhead conductors both in the steady as well as in the unsteady state. The simpler steady-state model implements equation 3 and returns the conductor's ampacity for given values of ambient temperature, solar radiation, wind speed and direction. On the other hand, the dynamic model is based on the differential equation 4, with the conductor temperature being the state variable. Figure 10 shows the principal structure of the model.

Usually, dynamic calculations of overhead lines are preformed in order to ensure that the conductor's temperature will not exceed the corresponding threshold in case of high fault currents with limited duration. The objective of such calculations is to determine the maximal clearance time for the fault. However, in this work dynamic modelling is implemented so as to examine the influence of fluctuating weather parameters on conductor temperature in the short term. The objective now is to evaluate on a probabilistic way the maximal (constant) current which can be carried by the line over a short time interval (one hour) without violating the temperature limit.

### A. *Evaluation of current constraint*

The problem setting is as follows: "Given a short-term forecast for all relevant weather parameters (solar radiation intensity, $I_S$, ambient temperature, $T_{amb}$, wind speed and direction, $v_w$ and $\theta_w$), calculate the maximal constant current, $I_{max}$, so that the conductor's temperature, $T_{av}$, does not exceed the respective threshold *at any time* within the forecast horizon". For this purpose, following algorithm has been implemented:

1) For each weather variable, randomly evaluate a time series for the forecast horizon using the probability density function (as calculated in section II) and the respective forecasted value. In particular, six random values (each for a time interval of 10 minutes) are calculated for the one-hour forecast horizon. For the reasons discussed in section II-B only the parameter wind speed has been modelled in detail; all other parameters are assumed to remain constant.
2) Calculate the steady-state thermal rating from equation 3 as initial value.

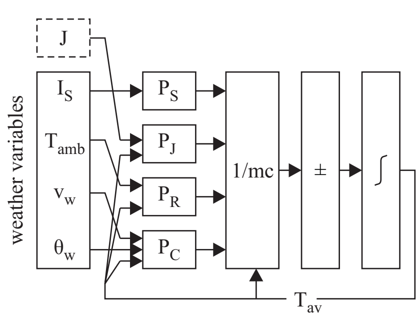


Fig. 10. Overview of the dynamic thermal model

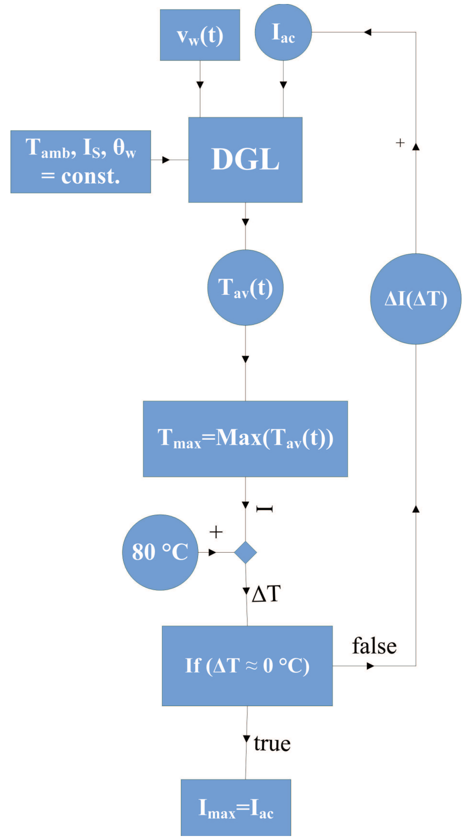


Fig. 11. Flowchart of the algorithm as applied to the case study of section IV

3) Simulate the conductor's temperature over the forecast horizon by means of the model in figure 10. The input time series for the weather variables have been calculated in step 1.
4) Identify the maximal temperature throughout the simulated time interval. Compare this value to the threshold: if it exceeds the threshold value, reduce the applied current accordingly. On the other hand, if the maximal temperature value lies beneath the threshold, increase the current.
5) Repeat steps 3 to 4 until the maximal conductor temperature falls into the range $[(1-\epsilon)T_{thres}; T_{thres}]$, with $T_{thres}$ being the threshold value for the conductor's temperature and $\epsilon$ a convergence factor. Store the so-calculated value for the current.
6) Repeat steps 1 to 5 for a large number of iterations. Finally, perform statistical analysis of the evaluated results (Monte Carlo simulation).

Figure 11 provides the flow chart of the described algorithm as applied to the case study of section IV.

## IV. Case study and results

After introducing the input data for the weather parameters and the simulation model in section II and III respectively, a case study will now be presented. An 429-AL1/56-ST1A steel reinforced aluminum conductor as standardised in [8] has been considered; its temperature threshold lies at 80°C.

Table I gives an overview of the one-hour forecasts for ambient temperature and global solar radiation. This case study does not consider a specific overhead line, thus the angle of attack has been assumed to be constant and equal 45°. In a more realistic study, the angle of attack has to be determined from the orientation of the line and the relative wind direction. Furthermore, some initial condition for the conductor's temperature is necessary in order to solve the differential equation 4. For this reason, a carried current of 600A has been assumed at $t_0$. This current, however, only defines the initial conductor temperature and is not further relevant for calculating the ampacity of the line.

TABLE I
PARAMETERS FOR THE CASE STUDY

| | |
|---|---|
| ambient temperature $T_{amb}$ | 25°C |
| global solar radiation $I_S$ | 900W/m$^2$ |
| angle of attack $\theta_w$ | 45° |
| initial current $I_{ac}$ | 600A |

Following simulation parameters have been used:

- Convergence factor $\epsilon$. Ampacity calculation was terminated as soon as the maximal conductor temperature lied in the following range: $[79,5°C; 80°C]$ (compare step 5 in section III-A).
- Number of total iterations, $n$. For each wind speed class 1000 iterations have been performed for the probabilistic analysis. In order to justify this setting, a comparative simulation with 20000 iterations has been performed for a single wind speed class; the calculated probability functions were almost identical for both settings.

### A. Results

The results of the probabilistic analysis are shown in figures 12 and 13. Only the weather variable wind speed has been modelled in a probabilistic way, all other parameters have been assumed as constant within the forecast horizon.

In figure 12 the minimum and maximum values of the 1000 calculated ampacities are depicted for each wind speed class. The blue dot describes the corresponding mean value. Furthermore, the steady-state thermal rating with weather conditions as defined in [8] is shown: its value amounts 892A. It is obvious that for all wind speed classes but the first (0m/s to 1m/s) the mean value of the calculated ampacity lies above the steady-state rating. Also, increasing wind speed leads –in average– to higher maximal ampacity, as expected.

Figure 13 shows the results in a quite different way: for each wind speed class, a probability function of the applicable ampacity has been estimated. It should be noted that the distribution functions are steeper for higher wind speeds. This is in agreement with the findings in section II-D, according to which the relative wind volatility decreases with increasing wind speed. Figure 13 may be used so as to identify any desired percentile of the maximal ampacity for a given wind speed class. For example, the 95-percentile specifies the current value, which will not lead to temperature violations with a probability of 95%.

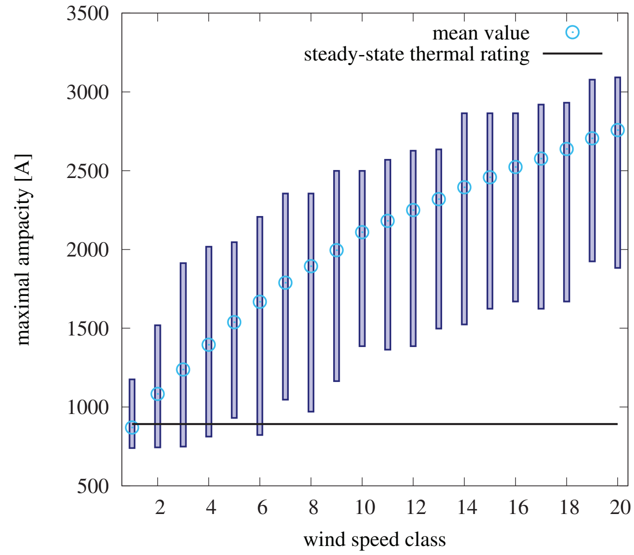


Fig. 12. Maximal ampacity for the different wind speed classes

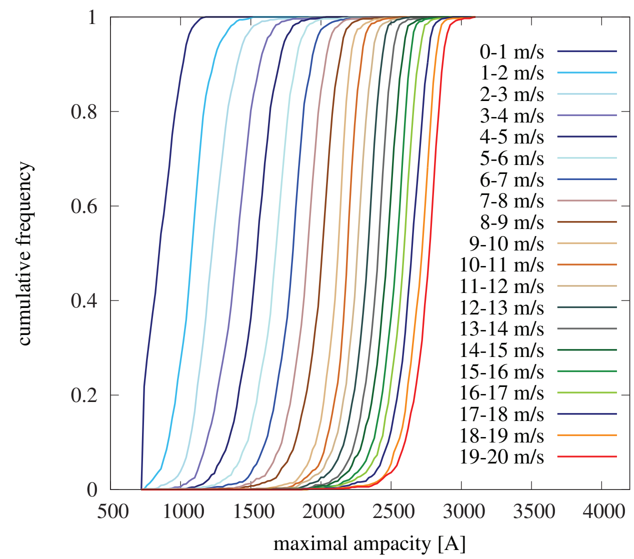


Fig. 13. Probability functions of the calculated ampacity for the different wind speed classes

### B. Safety factors

In figure 12 the steady-state thermal rating for standardised weather conditions is given (horizontal line). However, it is also possible to use the steady-state approach for weather-based loading: in this case, all weather parameters as given by the short-term forecast are assumed to be constant within the forecast horizon. In figure 14 the steady-state approach is compared with the results of the dynamic model. It is obvious that the steady-state rating is higher than the dynamic rating, since the effect of fluctuating weather conditions (in this case of fluctuating wind speed) has been neglected.

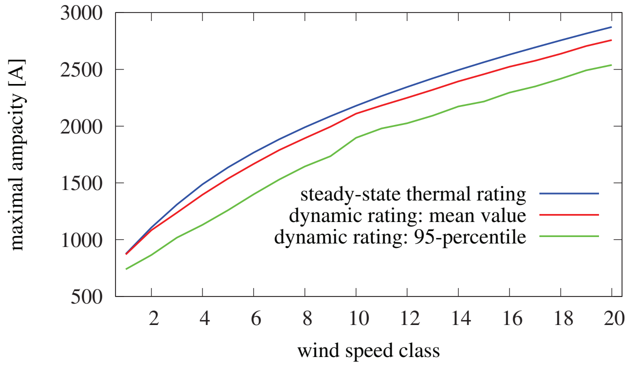


Fig. 14. Comparison of the steady-state and dynamic approach in weather-based loading

The gap between the steady-state and dynamic rating in figure 14 may be interpreted as uncertainty due to the fluctuation of weather conditions. In order to account for this uncertainty, appropriate safety factors can be determined: these factors should then be applied to the steady-state rating so as to reduce risk of overheating due to weather fluctuation (especially for this case study: due to wind speed fluctuation).

The safety factor for the $x^{\text{th}}$ wind speed class in defined as:

$$SF_x = \frac{I_{sx} - I_{dx}}{I_{sx}} \quad (6)$$

where $I_{sx}$ and $I_{dx}$ are the steady state and dynamic rating, respectively.

Figure 15 shows the calculated safety factors, in case the mean values or the 95-percentiles of the dynamic approach are considered. In the first case (mean values) scaling the steady-state rating 5% down would be sufficient. However, if the 95-percentile is considered, significant correction of the steady-state rating by up to 25% would be necessary.

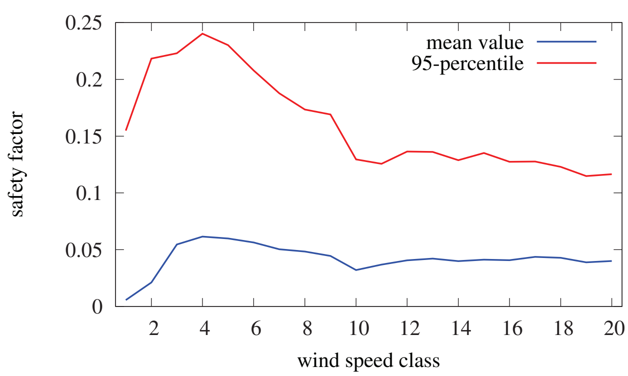


Fig. 15. Applicable safety factors for correction of the steady-state thermal rating

### C. Initial conditions

The results given in figures 12 and 13 base on the forecasted values of table I and the initial conductor temperature of approximately 33°C (this value results from the current at time $t_0$ of 600A). In case a higher initial conductor temperature is assumed, the applicable ampacity within the forecast horizon would be lower for all wind classes. Thus, the procedure described so far should be repeated for different initial conditions.

## V. Conclusions

The present work provides a comparison of the steady-state and dynamic approach to thermal rating of overhead lines for weather-based loading. In particular, the potential of using short-term weather forecasts rather than on-line measurements is addressed. However, when using forecasts the volatility of weather parameters within the forecast horizon may result in intermediate temperature violation if the steady-state rating is used on the basis of the forecasted values.

The presented procedure may help coping with this limitation. In a first step, time-series of the relevant weather parameters are analysed with regard to their volatility. Dynamic rating is provided by conductor temperature simulation on a probabilistic basis; a computer simulation model featuring the temperature models of Cigré and IEEE is implemented for this reason. Finally, the results from the steady-state and the dynamic approach are compared. For the considered case study, a safety factor of 25% should be applied to the steady-state thermal rating so as to reduce risk of overheating due to wind speed fluctuation.

## References

[1] Cigré Working Group 22.12, *Thermal behaviour of overhead conductors*, Cigré Brochure 207, August 2002

[2] IEEE Power Engineering Society, *Standard for calculating the current-temperature of bare overhead conductors*, IEEE Standard 738, November 2006

[3] Cigré Working Group B2.12, *Guide for selection of weather parameters for bare overhead conductor ratings*, Cigré Brochure 299, August 2006

[4] Cigré Working Group 22.12, *Probabilistic determination of conductor current ratings*, Cigré Electra, February 1996, No. 163, pp. 103-119

[5] Convenor R. Stephen, *Description of state of the art methods to determine thermal rating of lines in real-time and their application in optimising power flow*, Cigré Session 22, 2000, Paper No. 304

[6] H. Roman, G. Dangrieß, S. Dorendorf and T. Struck, *Freileitungsmonitoring im Hochspannungsnetz – Übertragungskapazität in Theorie und Praxis*, Energiewirtschaft, Vol. 108, No. 12, pp. 62-66

[7] M. Lange and U. Focken, *Studie zur Abschätzung der Netzkapazität in Mitteldeutschland in Wetterlagen mit hoher Windeinspeisung*, energy & meteo systems, Oldenburg, July 2008

[8] DIN EN 50182, *Conductors for overhead lines – Round wire concentric lay stranded conductors*, European Standard 50182:2001, German version, December 2001

[9] DIN EN 50326, *Conductors for overhead lines – Characteristics of greases*, European Standard 50326:2002, German version, January 2003

[10] A. Wasserrab, *Freileitungs-Monitoring – Untersuchung des dynamischen Temperaturverhaltens vom Leiterseil zur Mäßigung des stochastichen Charakters vom Wind*, Technische Universität Darmstadt, Bachelor thesis, April 2010

[11] BSH, Federal Maritime and Hydrographic Agency of Germany, *Research platform in North and Baltic sea FINO 1*, http://www.fino1.de, last visited: April 2010